THE JOURNAL OF BIOLOGICAL CHEMISTRY VOL. 285, NO. 53, pp. 41337–41347, December 31, 2010

Phosphatidylinositol 3-Kinase (PI3K) Signaling via Glycogen Synthase Kinase-3 (Gsk-3) Regulates DNA Methylation of Imprinted Loci*[S]

Received for publication, July 30, 2010, and in revised form, October 18, 2010 Published, JBC Papers in Press, November 3, 2010, DOI 10.1074/jbc.M110.170704

Anthony P. Popkie[‡], Leigh C. Zeidner[§], Ashley M. Albrecht[§], Anthony D'Ippolito[§], Sigrid Eckardt[§], David E. Newsom[¶], Joanna Groden[‖], Bradley W. Doble[**], Bruce Aronow[‡‡], K. John McLaughlin[§], Peter White[¶], and Christopher J. Phiel[‡§1]

From the [‡]Graduate Program in Molecular, Cellular and Developmental Biology, The Ohio State University, Columbus, Ohio 43210, the [§]Center for Molecular and Human Genetics and [¶]Center for Microbial Pathogenesis, The Research Institute at Nationwide Children's Hospital, Columbus, Ohio 43205, the [‖]Department of Molecular Virology, Immunology, and Medical Genetics, The Ohio State University College of Medicine, Columbus, Ohio 43210, the [**]McMaster Stem Cell and Cancer Research Institute, McMaster University, Hamilton, Ontario L8N 3Z5, Canada, and the [‡‡]Division of Biomedical Informatics, Cincinnati Children's Hospital, Cincinnati, Ohio 45229

Glycogen synthase kinase-3 (Gsk-3) isoforms, Gsk-3*α* and Gsk-3*β*, are constitutively active, largely inhibitory kinases involved in signal transduction. Underscoring their biological significance, altered Gsk-3 activity has been implicated in diabetes, Alzheimer disease, schizophrenia, and bipolar disorder. Here, we demonstrate that deletion of both *Gsk-3α* and *Gsk-3β* in mouse embryonic stem cells results in reduced expression of the *de novo* DNA methyltransferase Dnmt3a2, causing misexpression of the imprinted genes *Igf2*, *H19*, and *Igf2r* and hypomethylation of their corresponding imprinted control regions. Treatment of wild-type embryonic stem cells and neural stem cells with the Gsk-3 inhibitor, lithium, phenocopies the DNA hypomethylation at these imprinted loci. We show that inhibition of Gsk-3 by phosphatidylinositol 3-kinase (PI3K)-mediated activation of Akt also results in reduced DNA methylation at these imprinted loci. Finally, we find that N-Myc is a potent Gsk-3-dependent regulator of *Dnmt3a2* expression. In summary, we have identified a signal transduction pathway that is capable of altering the DNA methylation of imprinted loci.

Gsk-3[2] is functionally defined as the aggregate activity of both Gsk-3α and Gsk-3β isoforms that are encoded at distinct genetic loci. These highly redundant kinases are constitutively active and generally play an inhibitory role in the signal transduction pathways that they regulate (1), such as insulin signaling and canonical Wnt signaling (2). In addition, Gsk-3 has a major role in regulating differentiation of embryonic stem cells (3) and neural progenitors (4). Both insulin and Wnt signaling have been implicated in the regulation of stem cell pluripotency (5–13). Insulin signaling modulates Gsk-3 activity via the activity of upstream effectors; insulin or insulin-like growth factor binds to the insulin receptor, resulting in the activation of PI3K, which in turn phosphorylates and activates Akt (also called protein kinase B; PKB) (14). Akt subsequently phosphorylates several substrates, including Gsk-3 isoforms, on N-terminal serine residues (Gsk-3α Ser-21/Gsk-3β Ser-9), resulting in the inhibition of Gsk-3 activity (15).

Gsk-3 activity also represents a key regulatory step in the canonical Wnt signaling pathway. In the absence of ligand, a subset of cytoplasmic Gsk-3 is found in a protein complex that facilitates Gsk-3-mediated phosphorylation of β-catenin, targeting the protein for ubiquitination and degradation via the 26 S proteasome and keeping the Wnt pathway repressed (16). Upon ligand binding to the Wnt co-receptors, Gsk-3 redistributes to the cell surface (17), rendering the β-catenin destruction complex non-functional, causing the accumulation and subsequent nuclear translocation of β-catenin protein, which leads to the transcription of Wnt target genes. Although activated insulin and Wnt signaling both inhibit Gsk-3 activity, the mechanism of inhibition is distinct for each pathway; Wnt signaling does not affect insulin signaling, and insulin signaling does not activate Wnt target genes (18, 19).

Gsk-3 function in the insulin and Wnt signaling pathways has been thoroughly investigated, and numerous substrates of Gsk-3 have been described (2), yet the downstream effects of such a widely influential enzyme likely extend beyond our current knowledge. Here, we present evidence of a novel role for Gsk-3 isoforms in the regulation of DNA methylation at imprinted loci in mouse embryonic stem cells (ESCs). The *de novo* DNA methyltransferase, *Dnmt3a2*, is down-regulated in *Gsk-3* double knock-out (DKO) ESCs, resulting in reduced DNA methylation and altered expression of imprinted genes.

* This work was supported, in whole or in part, by National Institutes of Health Grants P30 DK078392 and U54RR025216 (to B. A.), R01CA63517 (to J. G.), and R01AG031833 (to C. J. P.).

[S] The on-line version of this article (available at http://www.jbc.org) contains supplemental Table 1 and Figs. 1 and 2.

[1] To whom correspondence should be addressed: Center for Molecular and Human Genetics, The Research Institute at Nationwide Children's Hospital, 700 Children's Dr. W432, Columbus, OH 43205. E-mail: phiel.1@osu.edu.

[2] The abbreviations used are: Gsk-3, glycogen synthase kinase-3; Dnmt1, DNA methyltransferase 1; Dnmt3a, DNA methyltransferase 3a; Dnmt3a2, DNA methyltransferase 3a, isoform 2; ESC, embryonic stem cell; DMD, differentially methylated domain; DMR2, differentially methylated region 2; IAP, intracisternal A-particle; Igf2, insulin-like growth factor II; Igf2r, insulin-like growth factor II receptor; NSC, neural stem cells; qPCR, quantitative polymerase chain reaction; DKO, double knock-out; Tricine, *N*-[2-hydroxy-1,1-bis(hydroxymethyl)ethyl]glycine.

Inhibition of Gsk-3 activity with lithium mimics the effects of reducing DNA methylation in both wild-type ESCs and wild-type neural stem cells. Furthermore, inactivation of Gsk-3 via components of the insulin signaling pathway results in reduced DNA methylation at imprinted loci. Finally, microarray data reveal that N-*myc* mRNA is down-regulated in *Gsk-3* DKO ESCs. We provide data that demonstrate that a highly conserved N-Myc binding site in the *Dnmt3a2* promoter is required for normal expression, and we demonstrate that siRNA knockdown of N-Myc results in a decrease in *Dnmt3a2* expression. Therefore, we have identified a novel function for Gsk-3 isoforms as key regulators of the epigenome, and our results add a new perspective on the consequences of altering Gsk-3 activity.

EXPERIMENTAL PROCEDURES

Cell Culture—Feeder-free wild-type, *Gsk-3*$\alpha^{-/-}$, *Gsk-3*$\beta^{-/-}$, and *Gsk-3* DKO ESCs (3) were grown on gelatin-coated plates in high glucose DMEM (Invitrogen) supplemented with 15% fetal bovine serum (HyClone), 1× non-essential amino acids, 1× sodium pyruvate, 2 mM L-glutamine, 1× penicillin/streptomycin (Invitrogen), 55 μM 2-mercaptoethanol, and 1000 units/ml ESGRO (Millipore). Media was replenished every other day. Neural stem cells were isolated from 12.5 days postcoitum embryos using NeuroCult neural stem cells (NSC) proliferation media (StemCell Technologies) following the manufacturer's protocol.

Microarray Analysis—Integrity of total RNA was evaluated using capillary electrophoresis (Bioanalyzer 2100, Agilent) and quantified using a Nanodrop 1000 (Nanodrop, Wilmington, DE). Following confirmation of RNA quality, Ovation™ biotin RNA amplification and labeling system (NuGen Technologies, Inc., San Carlos, CA) was used to prepare amplified, biotin-labeled cDNA from total RNA following manufacturer's instructions. Briefly, first strand cDNA was synthesized from 25 ng of total RNA using a unique first strand DNA/RNA chimeric primer and reverse transcriptase. Following double strand cDNA generation, amplification of cDNA was achieved by utilizing an isothermal DNA amplification process that involves repeated SPIA™ DNA/RNA primer binding, DNA duplication, strand displacement, and RNA cleavage. The amplified SPIA™ cDNA was purified and subjected to a two-step fragmentation and labeling process. The fragmented/biotinylated cDNA content was measured in a ND-1000 spectrophotometer, and the quality was analyzed on an RNA 6000 Nano LabChip (Agilent) using an Agilent Bioanalyzer 2100.

For each array, 2.2 μg of cDNA was hybridized onto the GeneChips® mouse genome 430 2.0 array (Affymetrix Inc.), which contains ~39,000 transcripts. The sequences from which these probe sets were derived were selected from GenBank™, dbEST, and RefSeq. The sequence clusters were created from the UniGene data base (Build 107, June 2002) and then refined by analysis and comparison with the publicly available draft assembly of the mouse genome from the Whitehead Institute for Genome Research (Mouse Genome Sequencing Consortium (MGSC), April 2002). Hybridization was allowed to continue for 16 h at 45 °C followed by washing and staining of microarrays in a Fluidics Station 450 (Affymetrix Inc.). GeneChip arrays were scanned in a GeneChip Scanner 3000 (Affymetrix Inc.), and CEL files were generated from DAT files using the GeneChip® operating software (GCOS) software (Affymetrix Inc.). The probe set signals were generated using the RMA algorithm in ArrayAssist 3.4 (Stratagene) and were used to determine differential gene expression by pairwise comparisons. The genes that were altered by 2-fold either way and had a false discovery rate of <10% were sorted and used for further interpretation of the microarray data. Microarray data have been deposited in GEO (www.ncbi.nlm.nih.gov/geo) under accession number GSE20015.

Stable Expression of Dnmt3a2 and p110 in ESCs*—Mouse *Dnmt3a2* cDNA was subcloned into a modified pCAGEN plasmid (from Connie Cepko, Addgene plasmid 11160) with a preceding puromycin resistance gene and internal ribosomal entry site. The plasmid containing a constitutively active myristoylated mouse p110 subunit of PI3K (p110*) ((5); from Shinya Yamanaka, Addgene plasmid 15689) expressed a hygromycin resistance cassette. ES cells were transfected with either the Dnmt3a2 or the p110* expression constructs with Lipofectamine 2000 (Invitrogen) in serum-free Opti-MEM (Invitrogen). Cells were allowed to recover in non-selective ES cell media for 24 h, after which puromycin-resistant (Dnmt3a2) or hygromycin-resistant (p110*) cells were grown in ES cell media containing 1 μg/ml puromycin or 200 μg/ml hygromycin, respectively. Puromycin/hygromycin-resistant colonies were isolated after 14 days of selection and expanded in selective media.

Dnmt3a2 Reporter Assays—The *Dnmt3a2* promoter was cloned by PCR amplification from bacterial artificial chromosome clone 330c18 RPCI-24 library using primers described in supplemental Table S1. Amplification products were TOPO TA-cloned into pCR8GW (Invitrogen) and then transferred by LR reaction to Gateway-modified pGL3-Basic, pGLF (from Glenn Maston, University of Massachusetts). Mutagenesis of the N-Myc binding site was accomplished by using the QuikChange II site-directed mutagenesis kit (Stratagene) (supplemental Table S1). Plasmids containing the *Dnmt3a2* promoter constructs driving firefly luciferase were co-transfected into ESCs with pRL SV40 with Lipofectamine 2000 (Invitrogen) in serum-free Opti-MEM (Invitrogen). Cells were replated in a 24-well plate 24 h after transfection and then lysed 48 h after transfection, at which time firefly and *Renilla* Luciferase assays were performed according to the manufacturer's protocol (Biotium) in a Veritas microplate luminometer (Turner Biosystems). Three replicates were performed for each transfection.

Antibodies and Protein Expression Analysis—Protein expression was assayed by Western blotting. Cells were resuspended in lysis buffer (137 mM NaCl, 10 mM Tris, pH 7.4, 1% Nonidet P-40) containing protease inhibitor mixture (1:100 Sigma) and sonicated for 10 30-s pulses at 4 °C in a Bioruptor (Diagenode) on the highest setting. Lysates were electrophoresed (8–20 mg/lane) through 7.5% Tris/Tricine gels and transferred onto nitrocellulose membrane (Whatman BA85) at 100 V for 1 h. Blots were blocked for 1 h with 5% milk/TBST (150 mM NaCl, 50 mM Tris, pH 7.4, 0.1% Tween) and

incubated in primary antibody diluted in 5% milk or 5% BSA (N-Myc and c-Myc antibodies)/TBST for 16–18 h at 4 °C. Antibodies were used under the following conditions. Anti-tubulin mouse mAb clone B-5-1-2 (Sigma) was diluted 1:10,000; anti-Dnmt3a mouse mAb clone 64B1446 (IMGENEX) was diluted 1:250; and anti-GSK-3α/β mouse mAb clone 1H8 (Calbiochem), anti-phospho-GSK-3α/β (Cell Signaling antibody 9331), anti-N-Myc (Cell Signaling antibody 9405), anti-c-Myc D84C12 XP (Cell Signaling antibody 5605), anti-PI3kinase p110α subunit C73F8 (Cell Signaling antibody 4249), anti-Akt1 2H10 (Cell Signaling antibody 2967), and anti-phospho-Akt Ser-473 193H12 (Cell Signaling antibody 4058) were all used at a 1:1000 dilution. Blots were incubated in anti-mouse or anti-rabbit IgG HRP secondary antibody (GE Healthcare) diluted 1:5000 in 5% milk in TBST for 45 min. Proteins were visualized using ECL detection reagent (GE Healthcare). Blots were stripped in a buffer consisting of 2% SDS, 62.5 mM Tris HCl, pH 6.7, and 100 mM β-mercaptoethanol at 50 °C for 30 min followed by repeated rinsing with TBST prior to reprobing with antibody.

DNA Isolation—High molecular weight genomic DNA was isolated after ESCs were washed in PBS and resuspended in lysis buffer (100 mM NaCl, 10 mM Tris, pH 8.0, 25 mM EDTA, pH 8.0, 0.5% SDS) and lysed 16–18 h at 55 °C. An equal volume of phenol:chloroform:isoamyl alcohol was added and gently rotated at ambient temperature for 2–3 h. DNA was precipitated with 2 volumes of ethanol and 0.1 volumes of sodium acetate, washed in 70% ethanol, and resuspended in sterile water.

Southern Blot—High molecular weight genomic DNA was digested with methylation-sensitive HpaII or methylation-insensitive MspI isoschizomers (New England Biolabs). Digested DNA was separated on 0.6% agarose in 0.5× Tris-acetate-EDTA and transferred to charged nylon membrane (Osmonics Inc.). The blot was hybridized with a [α-^{32}P]dCTP random primed labeled (Prime-It II, Stratagene) intracisternal A particle (IAP) probe (20) in FBI buffer (21) at 65 °C for 16 h, washed twice with 2× SSC + 0.1% SDS at 65 °C for 30 min, and imaged with a Typhoon 9400 PhosphorImager (GE Healthcare).

RNA Isolation—Cells were resuspended in TRIzol (Invitrogen), and RNA was isolated following the manufacturer's protocol and then further purified with the RNeasy RNA cleanup procedure (Qiagen).

cDNA Synthesis and Quantitative RT-PCR—Complementary DNA was synthesized with the High Capacity cDNA reverse transcription kit (Applied Biosystems) following the manufacturer's protocol. Quantitative RT-PCR was done on an Applied Biosystems 7500 using TaqMan® master mix and one of the following TaqMan assays (Applied Biosystems): Dnmt3a2 (Mm00463987_m1), Igf2 (Mm00439564_m1), H19 (Mm01156721_g1), Igf2r (Mm01313554_m1), Airn (Mm03943369_s1), Snrpn (Mm02391920_g1), N-Myc (Mm00476449_m1), or c-Myc (Mm00487803_m1). Three biological replicates and three technical replicates were used for each target analyzed. All threshold cycle (Ct) values were normalized to a mouse GAPDH endogenous control (Applied Biosystems), and relative quantitation was calculated from the median Ct value.

Bisulfite Sequencing—High molecular weight genomic DNA was fragmented by rapid freezing on dry ice and thawing at 42 °C for five repetitions. 500 ng of fragmented DNA was bisulfite-converted with the methyl code bisulfite conversion kit (Invitrogen) per the manufacturer's instructions. Igf2/H19 differentially methylated domain (DMD) and Igf2r differentially methylated region 2 (DMR2) were amplified from bisulfite-converted DNA with Platinum *Taq* (Invitrogen) using primers shown in supplemental Table S1 (22) and the following conditions: 94 °C for 10 min, 35 cycles of 94 °C for 45 s, 54 °C for 45 s, and 72 °C for 60 s followed by 72 °C for 7 min. PCR products were then TOPO TA-cloned into pCR8GW (Invitrogen). Plasmid clones were sequenced with M13 reverse primer (supplemental Table S1) using Big Dye version 3.1 chemistry with the following conditions: 96 °C for 10 s, then 25 cycles of 96 °C for 10 s, 50 °C for 5 s, and 60 °C for 4 min, and reaction products were resolved on an Applied Biosystems 3130XL genetic analyzer.

siRNA Transfection—125 pmol of Nmyc siRNA (Thermo SMARTpool L-058793-01-0005) or GFP siRNA (Dharmacon D-1300-20) was combined with 0.25 ml of Opti-MEM (Invitrogen). In parallel, 7.5 μl of Lipofectamine RNAiMAX (Invitrogen) was combined with 0.25 ml of Opti-MEM per transfection by gentle mixing. siRNA/Opti-MEM and RNAiMAX/Opti-MEM were then combined for a total volume of ~0.5 ml and incubated for 20 min at room temperature. This mixture was then used to resuspend a pellet of 1 million wild-type ESCs. The cell suspension was then plated into 2 ml of ESC media in an individual well of a gelatin-coated 6-well plate. Media was replaced with fresh ESC media the next day. At 72 h, cells were harvested, and protein and RNA were isolated as described above.

RESULTS

Expression of the de Novo DNA Methyltransferase Dnmt3a2 Is Reduced in Gsk-3 DKO ESCs—In an effort to better understand the downstream targets of Gsk-3, we performed microarray-based global gene expression analysis comparing wild-type (WT) mouse ESCs with those in which *Gsk-3α*, *Gsk-3β*, or both isoforms have been genetically deleted (*Gsk-3α*$^{-/-}$; *Gsk-3β*$^{-/-}$ DKO) (3). Inspection of our array data revealed a 6.2-fold down-regulation of the *de novo* DNA methyltransferase *Dnmt3a* in *Gsk-3* DKO ESCs but no effect in *Gsk-3α*$^{-/-}$ or *Gsk-3β*$^{-/-}$ ESCs (increased 1.1-fold in each). In addition to full-length Dnmt3a, there is a distinct smaller isoform, Dnmt3a2, which is transcribed from an alternative promoter within the *Dnmt3a* locus. Dnmt3a2 lacks the amino-terminal 219 amino acids found in Dnmt3a, but the remainder of the protein, including the domain containing methyltransferase activity, is identical between the isoforms (23). Importantly for this study, Dnmt3a2 is the isoform that is predominantly expressed in ESCs (24). The microarray probes are unable to differentiate between *Dnmt3a* isoforms, and the microarray expression data represent a composite of the expression of both *Dnmt3a* and *Dnmt3a2*. Therefore, we evaluated the protein expression of each individual isoform as the individual isoforms can be resolved by immunoblotting. We found that Dnmt3a2 protein expression is substantially reduced in *Gsk-3*

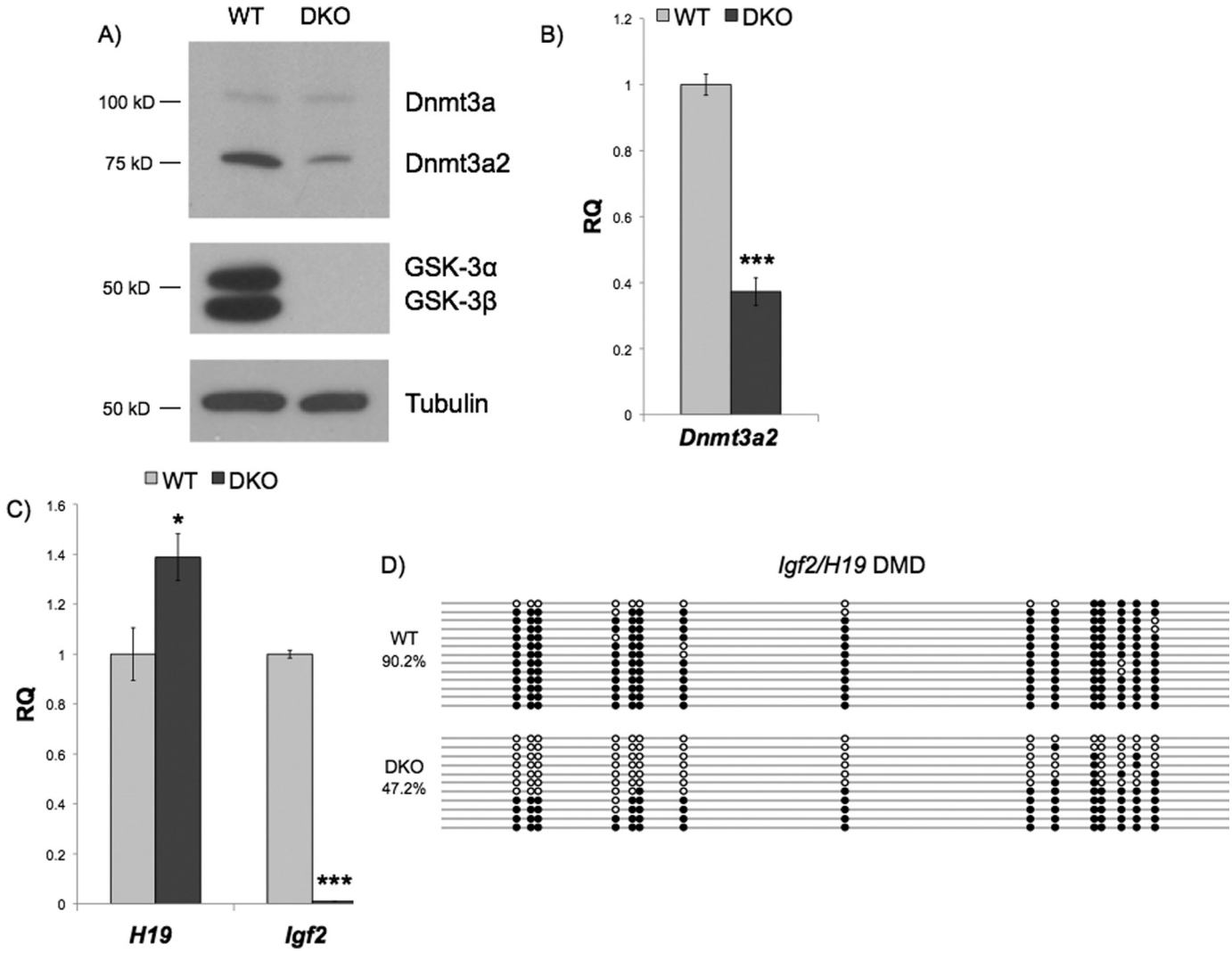

FIGURE 1. **Dnmt3a2 expression and DNA methylation are reduced in *Gsk-3* DKO ESCs.** *A*, Western blot of Dnmt3a isoforms in WT and *Gsk-3* DKO ESCs. Protein expression of Gsk-3 isoforms in WT and *Gsk-3* DKO ESCs is shown in the *middle panel*, whereas a Western blot for tubulin, which serves as a loading control, is shown in the *bottom panel*. *B*, real-time quantitative PCR of *Dnmt3a2* showing mRNA expression of *Dnmt3a2* in *Gsk-3* DKO ESCs relative to WT ESCs (*RQ* = relative quantitation). *Error bars* represent S.D. between biological replicates, $n = 3$ (***, $p < 0.001$, two-tailed *t* test). *C*, real-time quantitative PCR showing *H19* and *Igf2* mRNA expression in *Gsk-3* DKO ESCs relative to WT ESCs. *Error bars* represent S.D. between biological replicates, $n = 3$ (*, $p < 0.05$; ***, $p < 0.001$, two-tailed *t* test). *D*, bisulfite sequencing analysis of the *Igf2*/*H19* DMD. *Circles* represent 15 CpG dinucleotides analyzed within the *Igf2*/*H19* DMD. *Open circles* represent unmethylated CpG dinucleotides, whereas *filled circles* represent methylated CpG dinucleotides ($p < 0.01$, two-tailed *t* test).

DKO cells, whereas Dnmt3a protein levels were essentially unchanged (Fig. 1*A*). Real-time quantitative PCR (qPCR) revealed that mRNA expression of *Dnmt3a2* is reduced 2.7-fold in *Gsk-3* DKO ESCs when compared with WT ESCs (Fig. 1*B*).

Imprinted Loci Display Altered Gene Expression and DNA Methylation in Gsk-3 DKO ESCs—Dnmt3a/Dnmt3a2 activity is required for the establishment of DNA methylation at imprinted loci in germ cells (25). Mouse ESCs null for both *Dnmt3a* and *Dnmt3b* lose DNA methylation at imprinted loci after extended passaging, demonstrating a role for the *de novo* methyltransferases in the maintenance of DNA methylation at imprinted loci. Notably, re-expression of *Dnmt3a2* alone in *Dnmt3a*$^{-/-}$; *Dnmt3b*$^{-/-}$ ESCs is sufficient to fully restore DNA methylation at paternally imprinted loci, whereas re-expression of Dnmt3a or Dnmt3b1 is only able to minimally rescue DNA methylation at these loci (26). Based on these published observations, we hypothesized that reduction of *Dnmt3a2* expression in ESCs would result in the loss of DNA methylation and disruption of gene expression at imprinted loci. The imprinted locus containing the genes insulin-like growth factor II (*Igf2*) and *H19* has been well characterized. The reciprocal expression of *Igf2* and *H19* is regulated by a shared imprinting control region designated the DMD (27–29). In this imprinting control region, the paternal allele is methylated, resulting in expression of *Igf2* and silencing of *H19*, whereas conversely, the maternal allele is unmethylated, promoting *H19* expression while silencing *Igf2* (30). Indeed, the imprinted genes *H19* and *Igf2* display altered expression in *Gsk-3* DKO ESCs when compared with WT ESCs. *Igf2* and *H19* expression in *Gsk-3* DKO cells was assayed by qPCR, and *H19* expression is increased 1.4-fold, whereas *Igf2* expression is decreased 100-fold (Fig. 1*C*). This pattern of gene expression is consistent with a scenario for the loss of DNA methylation at the *Igf2*/*H19* DMD (29, 31, 32). We directly measured

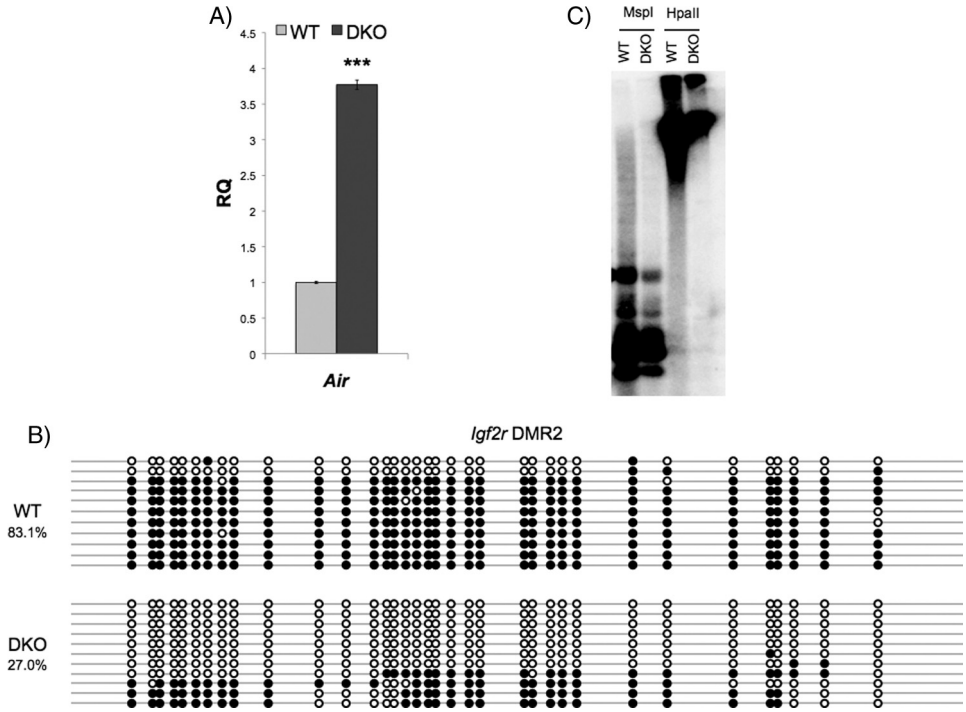

FIGURE 2. **Effect on DNA methylation in *Gsk-3* DKO ESCs extends to other imprinted genes but is not global.** *A*, real-time quantitative PCR analysis of *Air* mRNA expression in *Gsk-3* DKO ESCs relative to WT ESCs (*RQ* = relative quantitation). *Error bars* represent S.D. between biological replicates, $n = 3$. *B*, bisulfite sequencing analysis of the *Igf2r* DMR2 in WT and *Gsk-3* DKO ESCs. *Circles* represent 35 CpG dinucleotides analyzed within the *Igf2r* DMR2. *Open circles* represent unmethylated CpG dinucleotides, whereas *filled circles* represent methylated CpG dinucleotides ($p < 0.01$, two-tailed *t* test). *C*, Southern blot analysis showing methylation of IAP in WT and *Gsk-3* DKO ESCs. Genomic DNA from WT ESCs or *Gsk-3* DKO ESCs was digested with MspI or HpaII. MspI is not sensitive to DNA methylation and cuts DNA regardless of methylation status. HpaII is an isoschizomer of MspI that does not cut methylated DNA.

DNA methylation of the *Igf2*/*H19* DMD by bisulfite sequencing and found a 47% reduction of DNA methylation in *Gsk-3* DKO ESCs when compared with WT ESCs (Fig. 1*D*). These results strongly support the hypothesis that the alterations in *Igf2* and *H19* expression are due to a loss of DNA methylation at the *Igf2*/*H19* DMD.

Expression of *Air*, another imprinted gene that encodes for a long non-coding RNA (34), is increased in *Gsk-3* DKO ESCs. *Air* mRNA expression in *Gsk-3* DKO ESCs was assayed by qPCR and is increased by 3.8-fold (Fig. 2*A*). We then determined whether the change in expression of *Air* is due to a loss of DNA methylation. We performed bisulfite sequencing on DMR2 of *Igf2r*, from which *Air* is transcribed and known to be methylated on the maternal allele (22, 35). DNA methylation at DMR2 is reduced by 67% in *Gsk-3* DKO ESCs (Fig. 2*B*). These data suggest that the increase in *Air* expression is likely due to DNA hypomethylation within the *Igf2r* DMR2 and demonstrate that the loss of Gsk-3 activity on DNA methylation extends beyond the *Igf2*/*H19* DMD, supporting a possible broader role for Gsk-3 in the regulation of imprinted genes in the mouse.

Global DNA Methylation Is Unchanged in Gsk-3 DKO ESCs—We next determined whether the DNA hypomethylation we observed at imprinted loci is due to a defect in global DNA methylation. Because Dnmt1 is the primary enzyme responsible for maintaining genome-wide DNA methylation (36), we examined whether the loss of Gsk-3 activity affects Dnmt1 function. Repetitive DNA sequences, such as IAP repeats, are highly methylated in WT mouse ESCs (37) and largely unmethylated in $Dnmt1^{-/-}$ and *Dnmt1* hypomorph ESCs (38). IAP repeat methylation, although reduced, is largely retained in ESCs deficient in *de novo* DNA methyltransferase activity ($Dnmt3a^{-/-}$; $Dnmt3b^{-/-}$) (38, 39). Therefore, analyzing DNA methylation of IAP repeats provides an assay for Dnmt1 activity. Southern blotting using methylation-sensitive restriction enzymes revealed that *Gsk-3* DKO ESCs do not exhibit a significant difference in DNA methylation of IAP repeats when compared with wild-type ESCs (Fig. 2*C*), suggesting that there is not a general defect in DNA maintenance methylation in *Gsk-3* DKO cells. These data strengthen our hypothesis that the loss of DNA methylation observed at imprinted loci in *Gsk-3* DKO ESCs is likely the result of specific down-regulation of *Dnmt3a2* expression.

Ectopic Expression of Dnmt3a2 in Gsk-3 DKO ESCs Rescues the Deficits in DNA Methylation—To evaluate whether exogenous expression of *Dnmt3a2* could rescue the loss of DNA methylation at imprinted loci in *Gsk-3* DKO ESCs, we isolated puromycin-resistant *Gsk-3* DKO ESCs stably expressing *Dnmt3a2* under the control of the chicken β-actin (CAG) promoter and evaluated DNA methylation at the *Igf2/H19* DMD by bisulfite sequencing. A puromycin-resistant clone in which *Dnmt3a2* is stably overexpressed in DKO ESCs (Dnmt3a2) was selected for bisulfite sequencing analysis, and a puromycin-resistant clone that does not overexpress Dnmt3a2 (*Vector*) served as a negative control (Fig. 3*A*). Bisulfite sequencing of the *Igf2/H19* DMD revealed that DNA methylation is restored to levels previously observed in WT ESCs in the overexpressing clone (92.7%; Fig. 3*B*). Rescue of

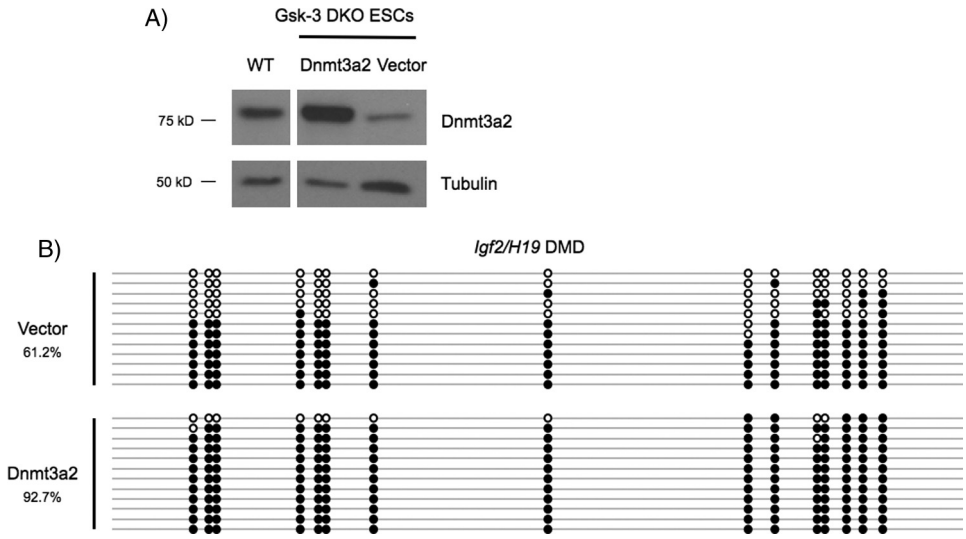

FIGURE 3. **Reintroduction of *Dnmt3a2* into *Gsk-3* DKO ESCs rescues DNA methylation.** *A*, Western blot of Dnmt3a2 expression in *Gsk-3* DKO ESCs stably expressing *Dnmt3a2* from the chicken β-actin (CAG) promoter (*Dnmt3a2*), DKO ESCs stably expressing the puromycin-resistant empty vector (*Vector*), and WT ESCs. The *WT*, *Dnmt3a2*, and *Vector lanes* are from the same blot, with intervening lanes removed. *B*, bisulfite sequencing of the *Igf2/H19* DMD in Dnmt3a2 rescued ESCs. *Open circles* represent unmethylated CpG dinucleotides, whereas *filled circles* represent methylated CpG dinucleotides.

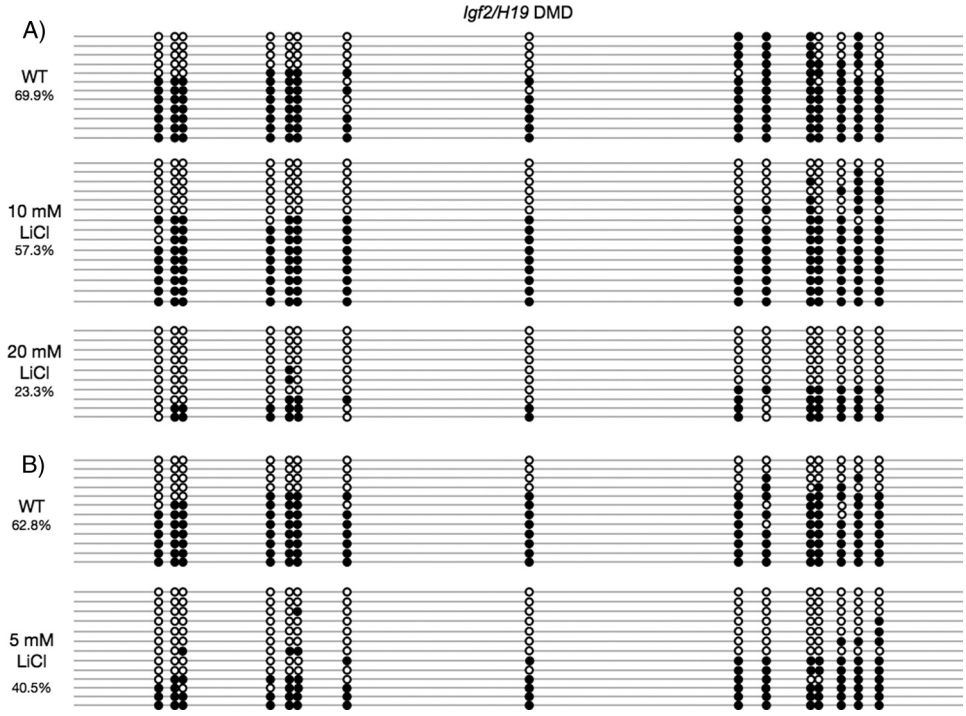

FIGURE 4. **Lithium inhibition of Gsk-3 results in hypomethylation.** *A*, WT ESCs were continuously grown in the presence of either 10 mM or 20 mM LiCl for 1 month. DNA methylation at CpG nucleotides within the *Igf2/H19* DMD was assessed by bisulfite sequencing (WT *versus* 20 mM LiCl, $p < 0.01$, two-tailed *t* test). *B*, DNA methylation of CpG nucleotides within the *Igf2/H19* DMD in WT NSCs that were continuously grown in the presence of 5 mM LiCl for 1 month ($p < 0.01$, two-tailed *t* test). *Open circles* represent unmethylated CpG dinucleotides, whereas *filled circles* represent methylated CpG dinucleotides.

the *Igf2*/*H19* DMD methylation defect by stably expressing *Dnmt3a2* in *Gsk-3* DKO ESCs strongly supports our hypothesis that reduced *Dnmt3a2* expression in *Gsk-3* DKO ESCs is the cause of decreased DNA methylation at imprinted loci.

Lithium Reduces DNA Methylation at Imprinted Loci—Based on the data obtained from *Gsk-3* DKO ESCs, we hypothesized that the Gsk-3 inhibitor lithium (40) should phenocopy the reduction in DNA methylation of imprinted genes. It was previously reported that *Dnmt3a*$^{-/-}$; *Dnmt3b*$^{-/-}$ ESCs required a high number of passages before a loss of DNA methylation was detected at imprinted loci (26). In light of this observation, we grew WT ESCs in the presence of lithium (40) for 4 weeks and then examined DNA methylation at the *Igf2/H19* DMD by bisulfite sequencing. Consistent with the reduction in DNA methylation in *Gsk-3* DKO ESCs, treatment of wild-type ESCs with lithium reduces DNA methylation at the *Igf2/H19* DMD in a dose-dependent manner. DNA methylation is reduced by 66% in wild-type ESCs treated with 20 mM lithium when compared with WT ESCs that had been cultured in parallel without lithium treatment (Fig. 4*A*).

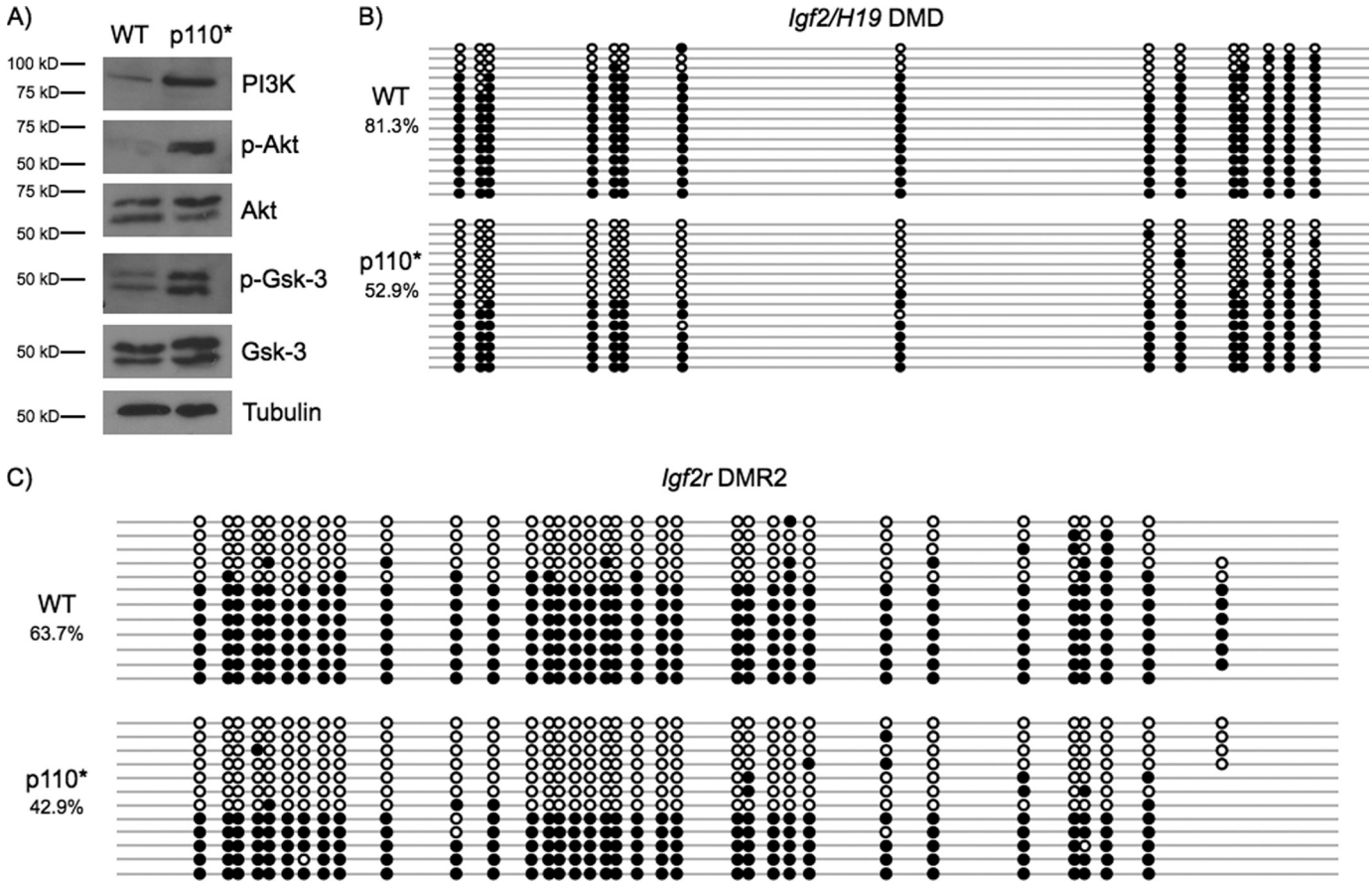

FIGURE 5. **Activation of components of the insulin signaling pathway reduces DNA methylation.** *A*, Western blots showing that WT ESCs stably transfected with p110* constitutively activate insulin signaling. *p-Akt*, phospho-Akt; *p-Gsk-3*, phospho-glycogen synthase kinase-3. *B*, bisulfite sequencing analysis of the *Igf2/H19* DMD in p110* ESCs when compared with WT ESCs ($p < 0.01$, two-tailed *t* test). *C*, bisulfite sequencing analysis of the *Igf2r* DMR2 in p110* ESCs when compared with WT ESCs. *Open circles* represent unmethylated CpG dinucleotides, whereas *filled circles* represent methylated CpG dinucleotides.

Next we examined the effect of Gsk-3 inhibitors on DNA methylation in a cell type other than ESCs. Because the Gsk-3 inhibitor lithium is used clinically to treat bipolar disorder, we chose to use cells from the neuronal lineage, specifically mouse NSC. After 4 weeks of growth in the presence of 5 mM lithium, we observed a 35% reduction in DNA methylation at the *Igf2/H19* DMD (Fig. 4*B*). These results demonstrate that the effect of lithium on DNA methylation extends to neural cells and expand the implications of our findings to other cell types.

Inactivation of Gsk-3 by PI3K results in Loss of DNA Methylation at Imprinted Loci—Activated insulin signaling negatively regulates Gsk-3 activity via inhibitory phosphorylation of an N-terminal serine by Akt (41). We investigated whether inactivation of Gsk-3 by constitutively active insulin signaling pathway could affect DNA methylation of imprinted genes. Expression of a myristoylated p110 subunit of PI3K (p110*) has previously been demonstrated to constitutively activate insulin signaling in ESCs (5). WT ESCs were stably transfected with p110*, and Western blots were performed to verify activation of the insulin pathway. Stable expression of p110* leads to robust phosphorylation of Akt on serine 473, which results in the activation of Akt. In addition, we found increased N-terminal phosphorylation of both Gsk-3α (serine 21) and Gsk-3β (serine 9), suggesting that the cellular pool of Gsk-3 regulated by Akt is inhibited (Fig. 5*A*). Bisulfite sequencing of the *H19/Igf2* DMD and *Igf2r* DMR2 demonstrated a substantial reduction of DNA methylation levels in p110* stable cells, similar to that seen in *Gsk-3* DKO ESCs (Fig. 5, *B* and *C*). These data demonstrate that activation of insulin signaling by constitutively active PI3K reduces DNA methylation at imprinted loci.

N-Myc Is a Potent Gsk-3-dependent Regulator of Dnmt3a2 Gene Expression—Our data show that the reduced levels of DNA methylation at imprinted loci in *Gsk-3* DKO ESCs are likely due to a decrease in *Dnmt3a2* levels. To establish the mechanism by which Gsk-3 activity regulates the expression of *Dnmt3a2*, we considered that both Dnmt3a2 mRNA and protein levels are decreased in Gsk-3 DKO ESCs, suggesting that the effect is likely due to altered transcriptional regulation. A role for miRNAs was excluded because both *Dnmt3a* and *Dnmt3a2* share a common 3′-untranslated region (UTR) yet are not equally affected by the loss of *Gsk-3* isoforms. Therefore, we focused on understanding the mechanism controlling *Dnmt3a2* transcription. A 1.9-kb fragment of the *Dnmt3a2* promoter was cloned (Fig. 6*A*), which is distinct from the regulatory regions of *Dnmt3a* and had previously been shown to be sufficient for driving high levels of reporter expression in ESCs (24). This 1.9-kb promoter fragment is capable of yielding robust (>35-fold) expression of a lucifer-

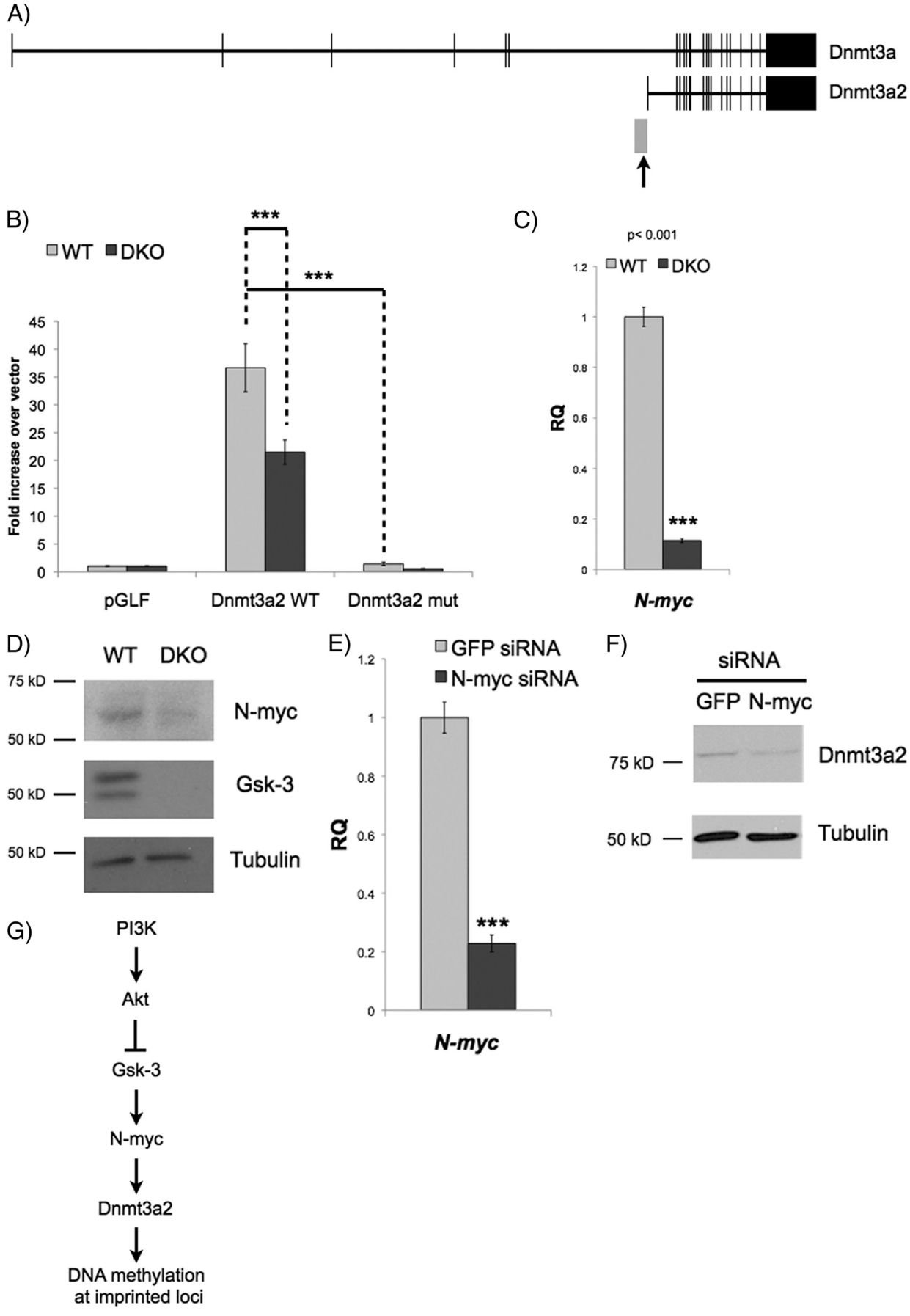
A)
Dnmt3a
Dnmt3a2
B)
WT DKO
***
***
Fold increase over vector
45
40
35
30
25
20
15
10
5
0
pGLF
Dnmt3a2 WT
Dnmt3a2 mut
C)
p< 0.001
WT DKO
RQ
1.2
1
0.8
0.6
0.4
0.2
0
***
N-myc
D)
WT DKO
75 kD
50 kD
N-myc
50 kD
Gsk-3
50 kD
Tubulin
E)
GFP siRNA
N-myc siRNA
RQ
1.2
1
0.8
0.6
0.4
0.2
0
***
N-myc
F)
siRNA
GFP N-myc
75 kD
Dnmt3a2
50 kD
Tubulin
G)
PI3K
Akt
Gsk-3
N-myc
Dnmt3a2
DNA methylation
at imprinted loci

ase reporter in WT ESCs (Fig. 6*B*). The reporter also recapitulates the effect of *Gsk-3* deletion on *Dnmt3a2* mRNA, showing an ~40% reduction in reporter activity when transfected into *Gsk-3* DKO ESCs.

In silico analysis of the *Dnmt3a2* promoter revealed a region of highly conserved sequence just proximal to the exon unique to *Dnmt3a2*, which encodes the 5′-UTR. Within this conserved region is a putative Myc binding site. Our microarray data showed a 2.8-fold decrease in N-Myc levels in *Gsk-3* DKO ESCs. Real-time qPCR revealed an 8.8-fold decrease in N-*myc* mRNA (Fig. 6*C*), and Western blot analysis confirmed the corresponding decrease in N-Myc protein levels (Fig. 6*D*). To test the importance of the Myc binding site in the *Dnmt3a2* promoter, we performed site-directed mutagenesis on the putative Myc binding site in the context of the 1.9-kb promoter fragment and transfected this reporter into ESCs. We observed a complete loss of reporter activity, confirming the functional importance of this binding site (Fig. 6*B*). Finally, transfection of WT ESCs with N-*myc* siRNA resulted in a 77% reduction in N-Myc levels (Fig. 6*E*) and a decrease in Dnmt3a2 protein (Fig. 6*F*), confirming the importance of N-Myc on the regulation of Dnmt3a2 in ESCs.

DISCUSSION

Mechanisms to explain how extracellular environmental signals are transduced to the nucleus to affect epigenetic modifications, such as DNA methylation, have been elusive (44). Here, we provide evidence for a novel role for Gsk-3 in the epigenetic regulation of imprinted genes. In mouse ESCs, deletion of Gsk-3 isoforms or expression of myristoylated PI3-kinase both lead to constitutive activation of downstream components of the insulin pathway, ultimately resulting in attenuated DNA methylation of imprinted loci. Although we provide evidence that several imprinted genes are hypomethylated as a consequence of the loss of Gsk-3 activity, it remains to be determined whether DNA methylation is reduced at all known imprinted loci in *Gsk-3* DKO ESCs or whether the effect on DNA methylation extends to non-imprinted genes.

Interestingly, we observed that ~90% of CpG dinucleotides analyzed in the *Igf2*/*H19* DMD were methylated in WT ESCs. It is expected that the number of methylated CpG dinucleotides would be closer to 50% for this imprinted locus because we did not discriminate between alleles in our bisulfite sequencing assay. The high amount of DNA methylation observed in WT ESCs is not likely due to PCR bias in our bisulfite sequencing procedure as we observed 44% methylation of the *Igf2*/*H19* DMD in NSC derived from WT mice using the same bisulfite sequencing assay (supplemental Fig. 1). It has been reported that cultured ESC lines may exhibit almost complete methylation of the *Igf2*/*H19* DMD on both parental alleles (33). In light of these previously reported observations, it is likely that the high degree of DNA methylation we detect at the *Igf2*/*H19* DMD in WT ESCs is due to biallelic methylation.

Our data show an increase in N-terminal phosphorylation of Ser-9/Ser-21 on Gsk-3 isoforms upon ectopic expression of PI3K, resulting in decreased DNA methylation at the *Igf2/H19* imprinting control region. Although our experimental approach utilized constitutively active PI3-kinase as a means of inducing phosphorylation on Gsk-3α Ser-21/Gsk-3β Ser-9, signal transduction of several pathways, such as protein kinase A (PKA) (45), also result in Gsk-3α Ser-21/Gsk-3β Ser-9 phosphorylation. Therefore, our data predict that signaling pathways that lead to the phosphorylation and inhibition of Gsk-3 akin to insulin signaling would lead to decreased DNA methylation at imprinted loci. We have not ruled out the possibility that inactivation of Gsk-3 by Wnt signaling can lead to hypomethylation of *Igf2/H19*. Further investigation is needed to determine whether activation of the Wnt pathway has the same effect on *Dnmt3a2* expression.

The deficits we observe in DNA methylation are due to reduced levels of the *de novo* DNA methyltransferase *Dnmt3a2*. Dnmt3a2 co-purifies with Dnmt3L in ES cells, whereas Dnmt3a does not (46, 47). Although Dnmt3L is catalytically inactive, it is required for establishment of DNA methylation at imprinted loci (48, 49) and recruits Dnmt3a2 to DNA sequences associated with unmethylated lysine 4 of histone H3 (47). *Dnmt3L* levels were not significantly changed in *Gsk-3* DKO ESCs (decreased 1.3-fold). These findings suggest that Dnmt3a2 plays a prominent role in the maintenance of DNA methylation at imprinted genes in early development. Heretofore, understanding the specific function of Dnmt3a2 *in vivo* has been difficult because targeted disruptions of the *Dnmt3a* locus in the mouse result in the simultaneous deletion of both *Dnmt3a* and *Dnmt3a2* as the isoforms share common 3′ exons. Our identification of a signal transduction pathway capable of specifically reducing levels of *Dnmt3a2* provides a new approach for the study of this isoform *in vivo*.

To better understand the mechanism by which *Dnmt3a2* mRNA is regulated, we cloned and analyzed a 1.9-kb fragment of mouse genomic DNA that contained a previously characterized promoter region. Computational analysis of the promoter revealed very little conservation of sequence across different species, with the exception of an ~200-bp region

FIGURE 6. **N-Myc regulates *Dnmt3a2* expression in a *Gsk-3*-dependent manner.** *A*, schematic representation of the locus encoding Dnmt3a isoforms. Exons are shown as the *vertical bars*. The *Dnmt3a2* promoter we used to drive the luciferase promoter is shown as the *gray box*. The *arrow* denotes the putative N-Myc binding site that we mutated in our reporter construct. *B*, *Dnmt3a2* promoter activity was assessed with a luciferase reporter. Reporters containing WT 1.9-kb *Dnmt3a2* promoter (WT) or promoter with two point mutations (*bases underlined*) in putative Myc binding site (CACGTG → CAGCTG; mutation (*mut*)) were transfected into WT and *Gsk-3* DKO ESCs. *Bars* represent -fold change over promoterless luciferase vector (*pGLF*). *Error bars* represent S.D. between replicate transfections, $n = 3$ (***, $p < 0.001$, two-tailed *t* test). *C*, real-time quantitative PCR analysis of N-*myc* mRNA expression in *Gsk-3* DKO ESCs relative to WT ESCs (*RQ* = relative quantitation). *Error bars* represent S.D. between biological replicates, $n = 3$ (***, $p < 0.001$, two-tailed *t* test). *D*, Western blots showing N-Myc, Gsk-3α, Gsk-3β, and tubulin in WT and *Gsk-3* DKO ESCs. *E*, real-time quantitative PCR analysis of N-*myc* mRNA expression in WT ESCs transfected with *GFP* siRNA and N-*myc* siRNA. *Error bars* represent S.D. between biological replicates, $n = 3$ (***, $p < 0.001$, two-tailed *t* test). *F*, Western blot for Dnmt3a2 in WT cells transfected with *GFP* siRNA and N-*myc* siRNA. *G*, model depicting a pathway that leads from PI3K activation to changes in DNA methylation in the nucleus.

just upstream of the novel *Dnmt3a2* exon. Within this region, we found a putative Myc binding site that is highly conserved, and a point mutation in this site completely impaired reporter activation. Recent chromatin immunoprecipitation-sequencing (ChIP-Seq) data showed that both c-Myc and N-Myc share an identical DNA binding motif (50); however, we did not observe a reduction in c-Myc protein in *Gsk-3* DKO ESCs. Furthermore, ChIP-Seq data in mouse ESCs show that N-Myc, but not c-Myc, binds specifically to the *Dnmt3a2* promoter (50). We have experimentally verified the importance of N-Myc on regulating Dnmt3a2 expression by knocking down N-*myc* via siRNA. Taken together with the decreased levels of N-Myc and unchanged levels of c-Myc (supplemental Fig. 2, *A* and *B*), we conclude that N-Myc regulates *Dnmt3a2* transcription. Gsk-3-mediated phosphorylation and degradation of c-Myc and N-Myc proteins by Gsk-3 have been reported in COS-7 cells (c-Myc) and cerebellar granule neuron precursors (N-Myc) (42, 43, 51). We did not observe this regulation of Myc proteins in our ESCs. In fact, we see an opposite effect of Gsk-3 on N-Myc expression and no effect on c-Myc expression. Our data likely reflect cell type-specific differences in the regulation of Myc proteins by Gsk-3. Furthermore, our real-time qPCR data indicate that N-Myc down-regulation in *Gsk-3* DKO ESCs is occurring at the level of transcriptional regulation. The mechanism by which Gsk-3 regulates N-*myc* transcription in ESCs remains to be determined.

The ability of the Gsk-3 inhibitor lithium to phenocopy the reduction in DNA methylation of imprinted genes seen in *Gsk-3* DKO ESCs is particularly intriguing. We have shown that DNA methylation is reduced at the *Igf2/H19* imprinting control region in both ESCs and NSCs after prolonged exposure to lithium. The effectiveness of lithium in the treatment of bipolar disorder was initially reported more than 60 years ago (52). Lithium has been widely prescribed ever since, although the therapeutic mechanism of action has not been fully defined. Growing evidence suggests that alterations in DNA methylation have a role in the development of bipolar disorder (53, 54). Our data raise the possibility that reduced DNA methylation of imprinted genes may be related to the mechanism of lithium action in bipolar disorder. It is noteworthy that another drug widely used for the treatment of bipolar disorder, valproic acid, also alters the epigenome by inhibiting histone deacetylase activity (55, 56). In the context of our findings, it is tempting to speculate that lithium and valproic acid are effective in treating bipolar disorder because they modify the expression of a common subset of genes via changes in DNA methylation and histone acetylation, respectively.

Our findings may also provide a new focus for the study of neurological diseases. Gsk-3 activity has been linked to schizophrenia (57), whereas alterations in the epigenome have been proposed to be a major factor in the development of schizophrenia (53). Of the postnatal tissues that have been examined to date, imprinting is clearly predominant in the brain, and alterations in these imprinting events have been shown to affect behavior (58). One example in humans is Prader-Willi syndrome, which is caused by a deletion on chromosome 15q11–13, an area that contains the imprinted genes *SNRPN* and Necdin (*NDN*) (59). This raises the possibility that altered Gsk-3 activity, resulting in aberrant DNA methylation of imprinted genes, could contribute to the development of schizophrenia or other behavioral disorders.

In summary, we have discovered a novel role for Gsk-3 in maintaining DNA methylation of imprinted loci in mouse ESCs. Because Gsk-3 is a nexus for numerous signal transduction pathways, the potential for Gsk-3 to regulate epigenetic changes could have profound consequences for our understanding of diverse human diseases.

Acknowledgments—We thank Drs. Jeff Kuret, Jing Yang, and Scott Harper for reading the manuscript and helpful discussions. We are also grateful to Dr. Glenn Maston for the pGLF construct, Dr. Carlos Miranda for assistance in isolating neural stem cells, and Dr. Yulei Wang for assistance with c-Myc qPCR.

REFERENCES

1. Force, T., and Woodgett, J. R. (2009) *J. Biol. Chem.* **284,** 9643–9647
2. Kockeritz, L., Doble, B., Patel, S., and Woodgett, J. R. (2006) *Curr. Drug. Targets* **7,** 1377–1388
3. Doble, B. W., Patel, S., Wood, G. A., Kockeritz, L. K., and Woodgett, J. R. (2007) *Dev. Cell* **12,** 957–971
4. Kim, W. Y., Wang, X., Wu, Y., Doble, B. W., Patel, S., Woodgett, J. R., and Snider, W. D. (2009) *Nat. Neurosci.* **12,** 1390–1397
5. Takahashi, K., Mitsui, K., and Yamanaka, S. (2003) *Nature* **423,** 541–545
6. Sato, N., Meijer, L., Skaltsounis, L., Greengard, P., and Brivanlou, A. H. (2004) *Nat. Med.* **10,** 55–63
7. Paling, N. R., Wheadon, H., Bone, H. K., and Welham, M. J. (2004) *J. Biol. Chem.* **279,** 48063–48070
8. Watanabe, S., Umehara, H., Murayama, K., Okabe, M., Kimura, T., and Nakano, T. (2006) *Oncogene* **25,** 2697–2707
9. Lu, J., Hou, R., Booth, C. J., Yang, S. H., and Snyder, M. (2006) *Proc. Natl. Acad. Sci. U.S.A.* **103,** 5688–5693
10. Storm, M. P., Bone, H. K., Beck, C. G., Bourillot, P. Y., Schreiber, V., Damiano, T., Nelson, A., Savatier, P., and Welham, M. J. (2007) *J. Biol. Chem.* **282,** 6265–6273
11. Miyabayashi, T., Teo, J. L., Yamamoto, M., McMillan, M., Nguyen, C., and Kahn, M. (2007) *Proc. Natl. Acad. Sci. U.S.A.* **104,** 5668–5673
12. Ying, Q. L., Wray, J., Nichols, J., Batlle-Morera, L., Doble, B., Woodgett, J., Cohen, P., and Smith, A. (2008) *Nature* **453,** 519–523
13. Niwa, H., Ogawa, K., Shimosato, D., and Adachi, K. (2009) *Nature* **460,** 118–122
14. Cantley, L. C. (2002) *Science* **296,** 1655–1657
15. Cross, D. A., Alessi, D. R., Cohen, P., Andjelkovich, M., and Hemmings, B. A. (1995) *Nature* **378,** 785–789
16. MacDonald, B. T., Tamai, K., and He, X. (2009) *Dev. Cell* **17,** 9–26
17. Zeng, X., Tamai, K., Doble, B., Li, S., Huang, H., Habas, R., Okamura, H., Woodgett, J., and He, X. (2005) *Nature* **438,** 873–877
18. Ding, V. W., Chen, R. H., and McCormick, F. (2000) *J. Biol. Chem.* **275,** 32475–32481
19. Ng, S. S., Mahmoudi, T., Danenberg, E., Bejaoui, I., de Lau, W., Korswagen, H. C., Schutte, M., and Clevers, H. (2009) *J. Biol. Chem.* **284,** 35308–35313
20. Dong, K. B., Maksakova, I. A., Mohn, F., Leung, D., Appanah, R., Lee, S., Yang, H. W., Lam, L. L., Mager, D. L., Schübeler, D., Tachibana, M., Shinkai, Y., and Lorincz, M. C. (2008) *EMBO J.* **27,** 2691–2701
21. Budowle, B., and Baechtel, F. S. (1990) *Appl. Theor. Electrophor.* **1,** 181–187
22. Yamasaki, Y., Kayashima, T., Soejima, H., Kinoshita, A., Yoshiura, K., Matsumoto, N., Ohta, T., Urano, T., Masuzaki, H., Ishimaru, T., Mukai, T., Niikawa, N., and Kishino, T. (2005) *Hum. Mol. Genet.* **14,** 2511–2520
23. Okano, M., Xie, S., and Li, E. (1998) *Nat. Genet.* **19,** 219–220

24. Chen, T., Ueda, Y., Xie, S., and Li, E. (2002) *J. Biol. Chem.* **277,** 38746–38754
25. Kaneda, M., Okano, M., Hata, K., Sado, T., Tsujimoto, N., Li, E., and Sasaki, H. (2004) *Nature* **429,** 900–903
26. Chen, T., Ueda, Y., Dodge, J. E., Wang, Z., and Li, E. (2003) *Mol. Cell. Biol.* **23,** 5594–5605
27. DeChiara, T. M., Robertson, E. J., and Efstratiadis, A. (1991) *Cell* **64,** 849–859
28. Bartolomei, M. S., Webber, A. L., Brunkow, M. E., and Tilghman, S. M. (1993) *Genes Dev.* **7,** 1663–1673
29. Tremblay, K. D., Duran, K. L., and Bartolomei, M. S. (1997) *Mol. Cell. Biol.* **17,** 4322–4329
30. Ideraabdullah, F. Y., Vigneau, S., and Bartolomei, M. S. (2008) *Mutat. Res.* **647,** 77–85
31. Jinno, Y., Sengoku, K., Nakao, M., Tamate, K., Miyamoto, T., Matsuzaka, T., Sutcliffe, J. S., Anan, T., Takuma, N., Nishiwaki, K., Ikeda, Y., Ishimaru, T., Ishikawa, M., and Niikawa, N. (1996) *Hum. Mol. Genet.* **5,** 1155–1161
32. Thorvaldsen, J. L., Duran, K. L., and Bartolomei, M. S. (1998) *Genes Dev.* **12,** 3693–3702
33. Dean, W., Bowden, L., Aitchison, A., Klose, J., Moore, T., Meneses, J. J., Reik, W., and Feil, R. (1998) *Development* **125,** 2273–2282
34. Lyle, R., Watanabe, D., te Vruchte, D., Lerchner, W., Smrzka, O. W., Wutz, A., Schageman, J., Hahner, L., Davies, C., and Barlow, D. P. (2000) *Nat. Genet.* **25,** 19–21
35. Stöger, R., Kubicka, P., Liu, C. G., Kafri, T., Razin, A., Cedar, H., and Barlow, D. P. (1993) *Cell* **73,** 61–71
36. Li, E., Bestor, T. H., and Jaenisch, R. (1992) *Cell* **69,** 915–926
37. Howlett, S. K., and Reik, W. (1991) *Development* **113,** 119–127
38. Okano, M., Bell, D. W., Haber, D. A., and Li, E. (1999) *Cell* **99,** 247–257
39. Lei, H., Oh, S. P., Okano, M., Jüttermann, R., Goss, K. A., Jaenisch, R., and Li, E. (1996) *Development* **122,** 3195–3205
40. Klein, P. S., and Melton, D. A. (1996) *Proc. Natl. Acad. Sci. U.S.A.* **93,** 8455–8459
41. Doble, B. W., and Woodgett, J. R. (2003) *J. Cell Sci.* **116,** 1175–1186
42. Gregory, M. A., Qi, Y., and Hann, S. R. (2003) *J. Biol. Chem.* **278,** 51606–51612
43. Sjostrom, S. K., Finn, G., Hahn, W. C., Rowitch, D. H., and Kenney, A. M. (2005) *Dev. Cell* **9,** 327–338
44. Berger, S. L., Kouzarides, T., Shiekhattar, R., and Shilatifard, A. (2009) *Genes Dev.* **23,** 781–783
45. Li, M., Wang, X., Meintzer, M. K., Laessig, T., Birnbaum, M. J., and Heidenreich, K. A. (2000) *Mol. Cell. Biol.* **20,** 9356–9363
46. Nimura, K., Ishida, C., Koriyama, H., Hata, K., Yamanaka, S., Li, E., Ura, K., and Kaneda, Y. (2006) *Genes Cells* **11,** 1225–1237
47. Ooi, S. K., Qiu, C., Bernstein, E., Li, K., Jia, D., Yang, Z., Erdjument-Bromage, H., Tempst, P., Lin, S. P., Allis, C. D., Cheng, X., and Bestor, T. H. (2007) *Nature* **448,** 714–717
48. Bourc'his, D., Xu, G. L., Lin, C. S., Bollman, B., and Bestor, T. H. (2001) *Science* **294,** 2536–2539
49. Kato, Y., Kaneda, M., Hata, K., Kumaki, K., Hisano, M., Kohara, Y., Okano, M., Li, E., Nozaki, M., and Sasaki, H. (2007) *Hum. Mol. Genet.* **16,** 2272–2280
50. Chen, X., Xu, H., Yuan, P., Fang, F., Huss, M., Vega, V. B., Wong, E., Orlov, Y. L., Zhang, W., Jiang, J., Loh, Y. H., Yeo, H. C., Yeo, Z. X., Narang, V., Govindarajan, K. R., Leong, B., Shahab, A., Ruan, Y., Bourque, G., Sung, W. K., Clarke, N. D., Wei, C. L., and Ng, H. H. (2008) *Cell* **133,** 1106–1117
51. Kenney, A. M., Cole, M. D., and Rowitch, D. H. (2003) *Development* **130,** 15–28
52. Cade, J. F. (1949) *Med. J. Aust* **2,** 349–352
53. Mill, J., Tang, T., Kaminsky, Z., Khare, T., Yazdanpanah, S., Bouchard, L., Jia, P., Assadzadeh, A., Flanagan, J., Schumacher, A., Wang, S. C., and Petronis, A. (2008) *Am. J. Hum. Genet.* **82,** 696–711
54. Kuratomi, G., Iwamoto, K., Bundo, M., Kusumi, I., Kato, N., Iwata, N., Ozaki, N., and Kato, T. (2008) *Mol. Psychiatry* **13,** 429–441
55. Phiel, C. J., Zhang, F., Huang, E. Y., Guenther, M. G., Lazar, M. A., and Klein, P. S. (2001) *J. Biol. Chem.* **276,** 36734–36741
56. Göttlicher, M., Minucci, S., Zhu, P., Krämer, O. H., Schimpf, A., Giavara, S., Sleeman, J. P., Lo Coco, F., Nervi, C., Pelicci, P. G., and Heinzel, T. (2001) *EMBO J.* **20,** 6969–6978
57. Mao, Y., Ge, X., Frank, C. L., Madison, J. M., Koehler, A. N., Doud, M. K., Tassa, C., Berry, E. M., Soda, T., Singh, K. K., Biechele, T., Petryshen, T. L., Moon, R. T., Haggarty, S. J., and Tsai, L. H. (2009) *Cell* **136,** 1017–1031
58. Wilkinson, L. S., Davies, W., and Isles, A. R. (2007) *Nat. Rev. Neurosci.* **8,** 832–843
59. Horsthemke, B., and Wagstaff, J. (2008) *Am. J. Med. Genet. A.* **146A,** 2041–52